# CORROSION BEHAVIOUR OF SINTER FORGED ALUMINUM COMPOSITES DURING HOT DEFORMATION

**S. Narayan[a, *]** **A. Rajeshkannan[b]** **RN. Deo[c]**

*** Corresponding Author**

**[a]Mr. SUMESH NARAYAN**

Assistant Lecturer, Mechanical Engineering,

School of Engineering and Physics,

Faculty of Science, Technology & Environment,

The University of the South Pacific, Laucala Campus,

PO Box 1168, Suva, FIJI.

Off. No. +679 3232034,

Fax No. +679 3231538,

Email: narayan_su@usp.ac.fj

**Co-Author**

[b]Dr. ANANTHANARAYANAN RAJESHKANNAN

Senior Lecturer, Mechanical Engineering,

School of Engineering and Physics,

Faculty of Science, Technology & Environment,

The University of the South Pacific, Laucala Campus,

PO Box 1168, Suva, FIJI.

Off. No. +679 3232695,

Fax No. +679 3231538,

Email: ananthanarayanan_r@usp.ac.fj

**Co-Author**

[b]Dr. RAVIN N DEO

Lecturer, Physics,

School of Engineering and Physics,

Faculty of Science, Technology & Environment,

The University of the South Pacific, Laucala Campus,

PO Box 1168, Suva, FIJI.

Off. No. +679 3232432,

Fax No. +679 3231511,

Email: deo_ra@usp.ac.fj

**Abstract**

A galvanostatic pulse technique was used to determine corrosion behavior of sinter-forged aluminium composites. Specimens were prepared using powder metallurgy (P/M) manufacturing techniques, with two different initial relative density and various carbide reinforcements such as titanium carbide (TiC), molybdenum carbide ($Mo_2C$), iron carbide ($Fe_3C$) and tungsten carbide (WC). The specimens were machined and molded in a thermo-plastic material so that a surface area of 1 $cm^2$ is exposed in a solution of 3.5wt% water solution of NaCl during the corrosion test. The corrosion behavior of the sinter-forged aluminium composites were studied alongside microstructure studies to expose corrosion dynamics and presented in this report.

**Keywords**: Corrosion; Galvanostatic; Aluminium composite; Powder metallurgy

## 1. Introduction

Carbide reinforced aluminium metal matrix composites are widely used in high strength industrial application due to low specific density, good wear resistance and low thermal expansion coefficient. SiC reinforced aluminium composites [1-2], TiC reinforced aluminium composites [3] and WC reinforced aluminium composites [4] have shown improved properties in aluminium metal matrix composites such as hardness, tool wear in turning, improvement in wear resistance and reduced corrosion rate. The presence of pores in the P/M parts especially open ones has significant effect on the corrosion resistance of sinter-forged aluminium composites. Wear and corrosion are the main reasons of P/M products failure in industry and these limit its application to corrosive and wear free environments. Solving these wear and corrosion problems will enhance the potential use of P/M parts for many industrial applications [5, 6].

Jinsun et al. [7] presented improved resistance of high strength Mg-Al-Mn-Ca magnesium alloy made by P/M process. They found that the SAWP process greatly improved the corrosion resistance due to dispersion of intermetallic phase. An emersion test method was used for the corrosion study. Dobrzanski et al. [8] conducted corrosion test using the measurement system consisting of the PG P-21 potentiostat working with the radiometer Copenhagen voltmeter 1 software. The corrosion behavior of varying composites was varying as well as the pitting amount and place on the exposed surface. Conventional electrochemical potentio-dynamics tests used by Marchiori et al. [9] in both cathode configuration and anode configuration to evaluate corrosion of plasma sintered unalloyed iron. Neubert et al. [10] studied mechanical properties and corrosion behavior of Al-Sc-Zr alloy prepared by P/M and reported the corrosion resistance and mechanical properties of Al-Sc-Zr is better than AA6061-T6 Al alloy. This was due to phase precipitation of $Al_3$ (Sc, Zr) particles during hot extrusion. Again they have used immersion test for 6 hours to determine the corrosion rate. Mamatha et al. [11] presented corrosion behavior of aluminium metal matrix composites reinforced with SiC particulates in HCl solution using weight loss method for 96 hours. The effect of varying SiC particulates in the aluminium composites on corrosion rate is evident. The corrosion resistance of iron P/M parts can be improved by surface treatment, nickel plating, coating, cathodic and anodic protection [12-13]. Steam treatment of sintered ferrous parts at $500^oC$ improves the hardness, wear and corrosion properties on the exposed surface due to the formation of thin $Fe_3O_4$ layer on the exposed surface

[14-15]. The effect of WC content on the microstructure and corrosion behavior of Ti (C, N) based cermets in nitric acid solution was studied by Chenghong et al. [16]. It was observed that WC is more easily oxidized and dissolved in nitric acid solution compared to Ti (C, N), hence, the corrosion rate of cermets increases and the corrosion resistance of Ti (C, N) based cermets decreases with increasing WC content.

The standard technique used for evaluating corrosion tests of P/M parts is immersion weight loss method [17-19]. Further, some of the immersion solutions used by several researchers are 3.5wt% NaCl solution, 1 M HCl solution, 9wt% $HNO_3$ solution, 0.5 M $KNO_3$ solution; however, the use of immersion solution is consistent throughout the whole experiment [20-22]. There are many non-destructive techniques (NDT) used such as linear polarization resistance (LPR) method [23], galvanostatic pulse technique [24], potentio-dynamic polarization test [7] and electrochemical impedance spectroscopy [25].

Currently no electrochemical process is well defined to measure the corrosion dynamics of aluminium metal matrix composites. Birbilis et al. [26] presented the problems encountered whilst using LPR method to study steel corrosion in concrete samples. They introduced a new technique to overcome problems encountered by other electrochemical process; the galvanostatic pulse technique. In this technique short galvanostatic pulse is used moving away from other technique using longer pulses with greater error [27]. Deo et al. [24] has successfully used this galvanostatic pulse technique successfully to study metal corrosion in different soils.

Based on the published literature, there is less information about the corrosion behavior of aluminium metal matrix composite with the effect of WC, $Mo_2C$ and $Fe_3C$ reinforcements. In the present study a galvanostatic pulse technique is used to evaluate the corrosion behavior of several aluminium metal matrix composites such as Al1TIC, Al2TiC, Al3TiC, Al4TiC, Al2$Fe_3C$, Al4$Fe_3C$, Al2$Mo_2C$, Al4$Mo_2C$, Al2WC and Al4WC. Further, the effect of initial porosity levels in aforementioned composites on corrosion resistance was also investigated and presented in this paper. A very similar method was used by Jinsun et al. [7] to study the corrosion behavior of magnesium alloy made by rapid solidification powder metallurgy process. They have used a

typical three electrode cell with a saturated Ag/AgCl reference, Pt counter and the specimen as the working electrode and same is used in our research work.

## 2. Aluminium composite/NaCl solution interface

A interface is formed when the aluminium composite comes in contact with the 3.5% NaCl water solution. This interface can be modelled by a equivalent circuit called the Randle's circuit. The circuit reassembles $R_pC_{dl}$ parallel arrangement in series with NaCl solution resistance, $R_\Omega$, whereby $R_p$ is the polarization resistance and $C_{dl}$ is the double layer capacitance shown in Fig. 1.a. The capacitance associated with the aluminium composite will vary depending on the reinforcements present in the composites. The double layer capacitance is non-ideal due to the β-parameter. β-parameter is an indicator of dispersion characteristics. It can be used to illustrate how the surface is taking part in the corrosion process. When β = 1, it indicates ideal uniform corrosion and $C_{dl}$ is an ideal capacitor. When β < 1, it indicates localized corrosion and $C_{dl}$ is a non-ideal capacitor.

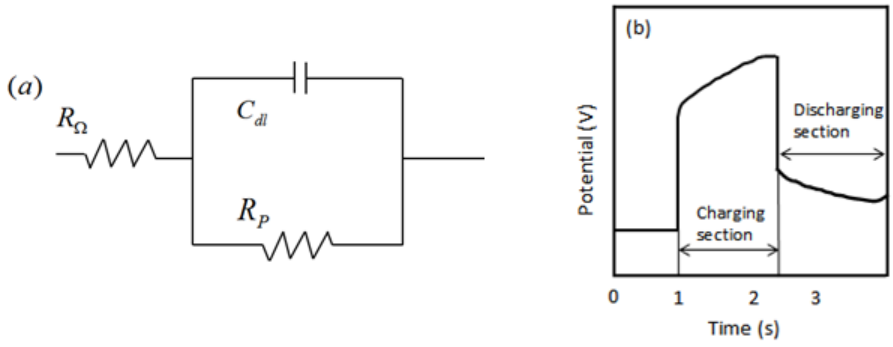


Figure 1: (a) Equivalent circuit diagram of the metal matrix composites/NaCl solution interface, (b) the Randle's type circuit used to model the interfacial response in this study.

## 2. Experimental Details

### *2.1 Specimen preparation*

The materials used in the current investigation are aluminium powder of 150 $\mu$m and titanium carbide, tungsten carbide, molybdenum carbide and iron carbide, of 50 $\mu$m. All powders used in the present investigation had purity levels of 99.7%.

The required amount of powders was mixed to obtain the aforementioned aluminium carbide composites using planetary ball milling machine. The ball mill was run for 2 hours at 200 rpm to get a homogenized mixture. The apparent density was continuously measured to ensure uniform distribution of the reinforcement particles in the matrix.

The powders corresponding to cylindrical specimens with diameter of 24 mm and height of 10 mm were compacted in a pressure range of 139 MPa to 159 MPa (hydraulic press) to obtain relative density of 0.86 ± 0.01 and 0.82 ± 0.01. The specimens were coated with $Al_2O_3$ mixed with acetone to avoid oxidation during the sintering process. The specimens were left for atmospheric drying for a period of 24 hours.

Then the specimens were sintered in an electric muffle furnace at 220$^{o}$C for 30 minutes and then at 594$^{o}$C for an additional period of 60 minutes. Each specimen was compressively deformed at a temperature of 594$^{o}$C to two different height strains. Finally the specimens were left for atmospheric cooling.

*2.2 Solution Preparation*

3.5% NaCl was prepared using analytical grade reagent and distilled water. Each specimen was immersed in 500 mls NaCl solution separately such that the ratio of exposed specimen surface area ($cm^2$) to volume of the NaCl solution (ml) was about 1:500.

*2.3 Microstructure*

The specimens for microstructure characterization were cut at the center with the observation plane parallel to the compression direction. The microstructures were examined using an optical microscope. The specimens were ground with 1200 grit emery and polished with 9 microns diamond paste, then with 3 microns diamond paste and finally with colloidal silica. Then the specimens were cleaned with distilled water and absolute ethanol and dried with warm flowing air. These specimens were then etched with Keller's reagent. These were then cleaned with distilled water then ethanol and dried with warm flowing air before microstructure examination.

To study the corrosion behavior at the initial stage, another set of specimens were ground with 1200 grit emery and polished with 9 microns diamond paste, then with 3 microns diamond paste and finally with colloidal silica. These specimens were then immersed in the 3.5% NaCl water

solution for 4 hours and the surface was observed with an optical microscope. The specimens were cleaned with distilled water, then with absolute ethanol and dried with warm flowing air.

*2.4 Electrochemical measurement*

A classical three electrode configuration was used with an Ag/AgCl reference electrode, platinum as counter electrode and the specimen as working electrode. All the specimens were machined to form cylinder of diameter of 1.13 cm. The specimens were then molded in a thermoplastic material to only expose a surface area of 1 $cm^2$. The exposed surface of the specimens for the test were ground using 1200 grit emery paper and cleaned with distilled water and absolute ethanol. A 2 mm hole was made into the thermoplastic material and a copper wire was inserted to just touch the specimen to allow galvanostatic pulse current flow. The hole was sealed with adhesive to hold the copper wire in place and to avoid the solution from entering. It was ensured that the exposed surface is not damaged. The Eco-chemie microAUTOLAB III potentiostat/galvanostat together with the General Purpose Electrochemical Software was used to supply short (1s) galvanostatic pulse and the resulting potential-time response was recorded internally by this set-up. The measurements were taken after 2 hours of immersion in 3.5% NaCl solution using a purpose-built inversion program. The counter and reference electrode were secured properly allowing contact with the solution. The depth of the immersion was kept constant. A potential of 1.5 V was supplied between the working and counter electrode for al the measurements. The potential circuit data's were then used to plot the charging and discharging curves along with the curve-fitting techniques to extract the corrosion related parameters. A purpose-built inversion program was also used for this analysis. The following parameters were obtained such as corrosion potential (Ecorr), β-parameter, polarization resistance ($R_p$) double layer capacitance ($C_{dl}$) and corrosion current density (Icorr) using the software program. A schematic of the experimental setup is given in Figure 2.

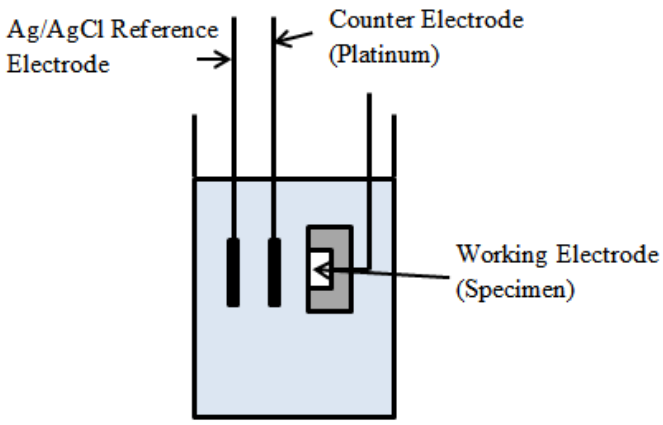


Figure 2: Illustration of the electrochemical setup in this study.

## 3. Results and Discussion

### *3.1 Microstructure*

To study the corrosion behavior at the initial stage, all specimens after the standard preparation technique as discussed in section 2.3 of this paper were immersed in 3.5% NaCl water solution for 4 hours and the surface was observed with an optical microscope. The specimens were cleaned with distilled water, then with absolute ethanol and dried with warm flowing air before microstructure viewing. Figure 3 gives the microstructural view of TiC reinforced aluminium and Figure 4 gives the micrographs of WC, $Fe_3C$ and $Mo_2C$ reinforced aluminium metal matrix composites. Apart from the varying carbide and varying carbide concentrations, initial relative density and final height strain is varied. A low height strain here is referred to as low deformed specimen and a higher height strain is referred to as a highly deformed specimen. Generally it was observed in most composites that lower initial relative density specimens showed poor materials resistance to corrosion. Further, low deformed specimens also showed poor materials resistance to corrosion. Specimens of 0.86 initial relative density and highly deformed specimens showed lower corrosion when compared to lower initial relative density and low deformed specimens. The presence of pores may act as the influencing factor here and lower initial relative density and low deformed specimens has higher number of pores present in the bulk material promoting corrosion. It is seen from the microstructures that corrosion is higher around the pores and also around the carbide reinforcement particles. The chemical reaction for corrosion is enhanced at the grain boundaries of two different materials, that is, respective carbides and aluminium. Further, from Figure 3 it can be seen that when the TiC content is increased in the

specimens the surface corrosion is reduced significantly, however, spot/localized corrosion is seen and is mainly around the reinforced particles. When the TiC particles are low the corrosion activity is mainly concentrated on the whole surface area. However, as the TiC particles increase the number of weaker grain boundaries is higher, between reinforced particle and aluminium particles, and the corrosion activity shifts to these weaker grain boundaries, promoting spot/localized corrosion. Also, pitting corrosion is enhanced in the highly deformed specimens as the TiC particles increases in the specimens. This is due to the surface variation due to presence of carbide reinforcements in composites can promote increased pitting corrosion.

From Figure 4 it can be stated that $Mo_2C$ reinforced aluminium composites showed highest corrosion irrespective of initial relative density, percentage carbide concentrations, or high or low deformation of the specimen compared to other composites. Extensive pitting corrosion is shown by these specimens. After $Mo_2C$ reinforced aluminium composites, TiC reinforced aluminium composites showed poor resistance to corrosion. Further, WC reinforced aluminium composite and $Fe_3C$ reinforced aluminium composite showed better material resistance to corrosion when compared to $Mo_2C$ and TiC reinforced aluminium composites. It can be concretely noted that $Mo_2C$ reinforced composites prepared by primary powder metallurgy manufacturing process has very poor material resistance to corrosion. Hence, parts prepared from this combination and process needs to be well protected to avoid corrosion in actual application. Pitting corrosion starts with the formation of pits. Pit initiation starts with the absorption of $Cl^-$ ions and its chemical reaction with the oxide film [28]. This phenomenon is high in $Mo_2C$ reinforced aluminium composites. Thus many corrosion pits exists damaging the hard particle bonds. This will lead to the falling of unsupported hard phase particles from the surface of the specimen promoting rapid corrosion.

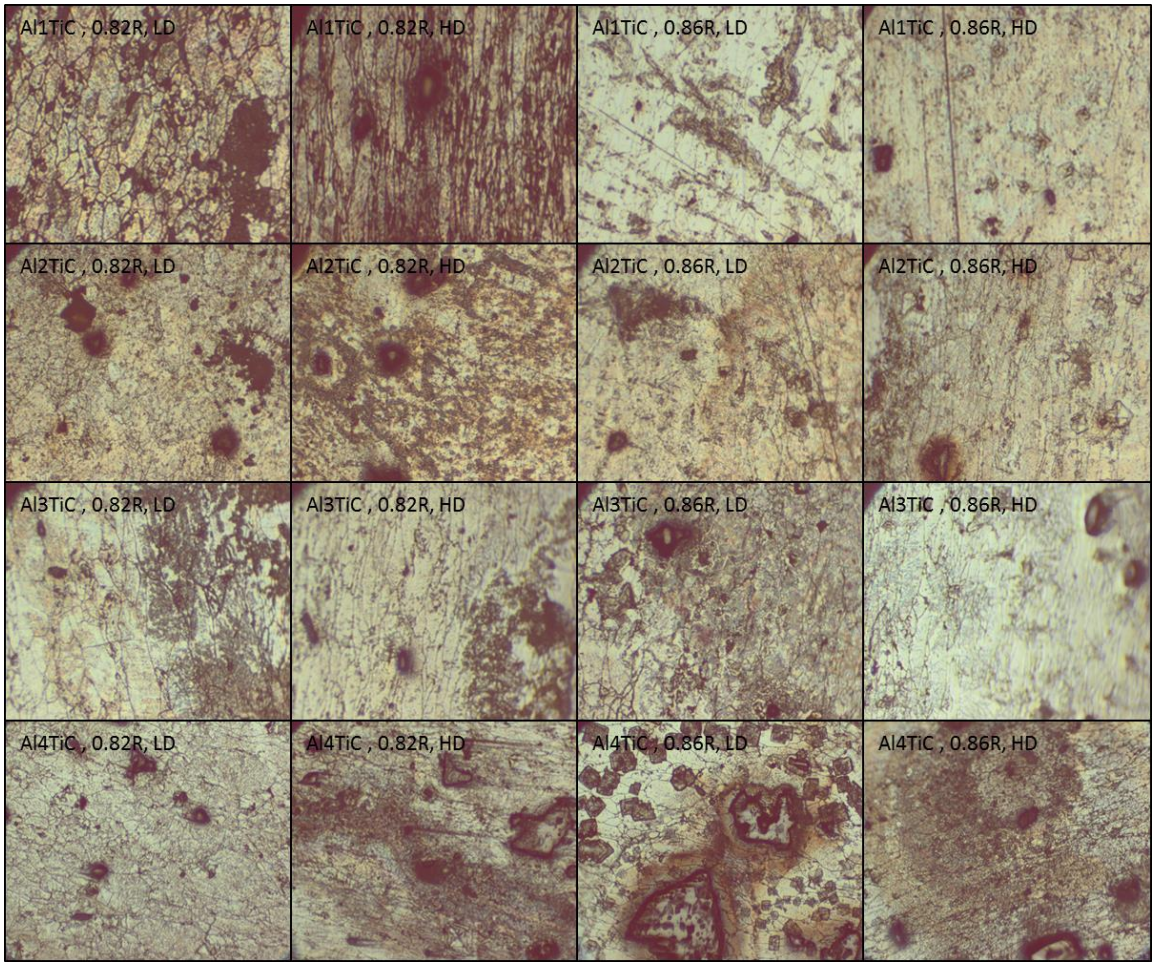


Figure 3: Micrographs of P/M TiC reinforced aluminium composites after immersion of 4 hours in 3.5%NaCl.

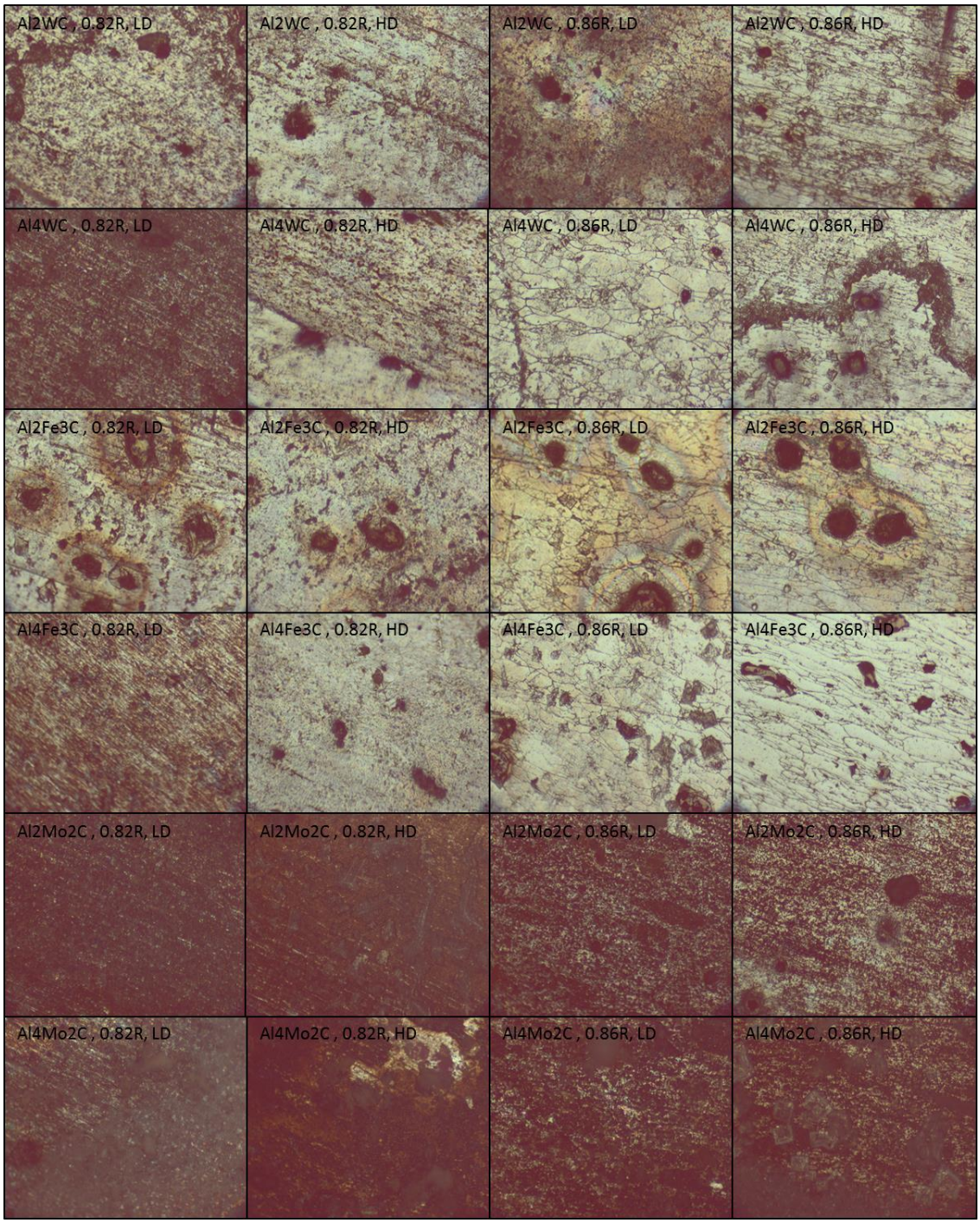


Figure 4: Micrographs of P/M WC, Fe3C, Mo2C reinforced aluminium composites after immersion of 4 hours in 3.5%NaCl.

### *3.2. Electrochemical measurements*

Results from short galvanostatic pulse measurements for different carbide reinforced aluminium are described here. Measurements were conducted at 2 hours after immersion in 3.5% NaCl

water solution. The galvanostatic pulse technique measures the following parameters, polarization resistance, $R_p$, double layer capacitance, $C_{dl}$, beta parameter, $\beta$, and corrosion potential, $E_{corr}$. The following parameters can be successfully used to access the corrosion behavior of the metals and calculate the corrosion rate. A simple electric circuit was implemented and the potential time response was measured after application of a short (1s) galvanostatic pulse. The details of this circuit are discussed in Deo [29]. A typical potential time response measured in this work is shown in Figure 5. It has two potential-time response period, first is the charging curve and the other is the discharging curve. The charging curve is modelled by a Randle's type circuit shown in Fig. 1. a.

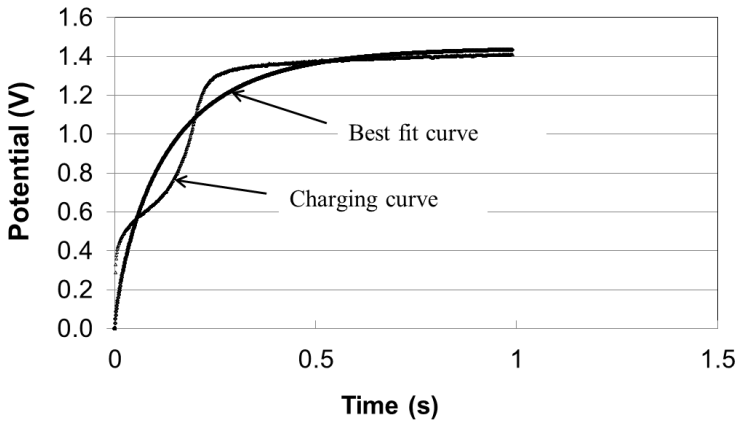


Figure 5: Potential time response of Al1TiC, charging curve with best fit curve.

The corrosion related parameters ($\beta$, $C_{dl}$, $R_p$, $E_{corr}$) and $R_\Omega$ can be determined either by analyzing the charging curve or the discharging curve. A purpose-built inversion program is used for the measurements and analysis of results for this work and the details of the program is discussed elsewhere [30]. An excellent feature of the purpose-built inversion program is that the corrosion parameters can be determined by just analyzing the charging curve without the need of the discharging curve. On the other hand, if discharging curve is used to obtain the results then the charging curve needs to be analyzed first as the discharging curve analysis requires some input from the charging curve. Hence, as we just need the corrosion parameters ($\beta$, $C_{dl}$, $R_p$, $E_{corr}$) only the charging curve is used for this work, the best curve fitting techniques is only applied to the charging curve using the purpose-built program with error bars.

An increase in polarization resistance, $R_p$, values and a decrease in double layer capacitance values, $C_{dl}$, indicate an increase in materials resistance to corrosion. Similar method and analysis is discussed by Birbilis et al. [31] to evaluate corrosion behavior of reinforced steels in concrete. Further, as the polarization resistance, $R_p$, increases the corrosion current decreases indication low corrosion. A higher $C_{dl}$ value indicates greater ability to store electric charge by the working electrode. This will create higher corrosion density indicating increased corrosion. It is noted that the distance between the reference electrode and the working electrode for all experimental work in this research is kept constant. Further, the test solution is also kept constant for all experimental works. Hence the $R_p$ and $C_{dl}$ values only depends on the variables tested in this research work which are carbide concentrations, height strain and initial relative density. Figure 6 gives the variation of $C_{dl}$ against $R_p$. A strong inverse relationship between $R_p$ and $C_{dl}$ in log-log plot is depicted from Figure 6. Hence, $R_p$ and $C_{dl}$ corrosion parameters can be effectively used to study the corrosion behavior. This galvanostatic pulse corrosion parameters, β, $C_{dl}$, $R_p$, is effectively used to study reinforced steel corrosion in concrete slabs [26-30]. The authors have effectively utilized β, $C_{dl}$, $R_p$ parameters to study corrosion behavior.

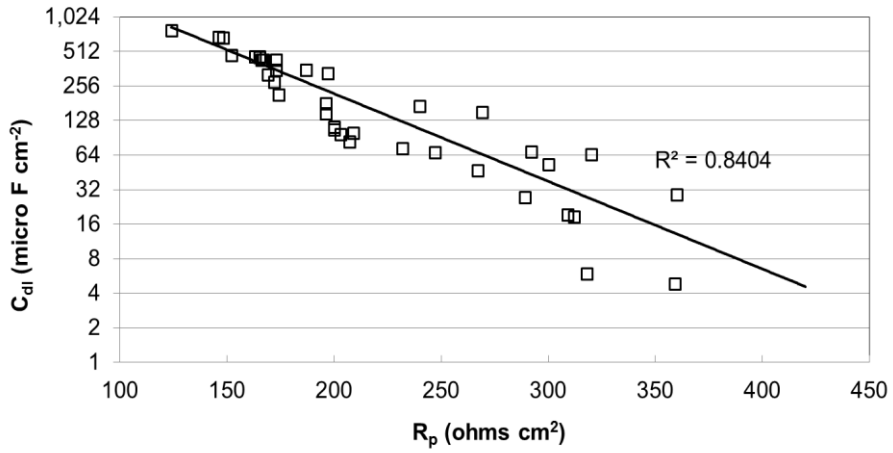


Figure 6: Variation between polarization resistance and double layer capacitance for different composites measured at 2 hours of immersion.

Figure 7 shows the variation of $R_p$ and $C_{dl}$ for the respective carbide reinforced aluminium tested in this research work. It can be seen (Fig. 7 (a and c)) that $R_p$ is found to be higher in Al2$Fe_3C$ followed by Al2WC, Al2TiC and lowest for Al2$Mo_2C$. At the same time $C_{dl}$ is found to be higher in Al2$Mo_2C$ and Al2TiC and lower in Al2WC and Al2$Fe_3C$. Al2$Fe_3C$ and Al2WC

showed greater material resistance to corrosion as Al2TiC and Al2 $Mo_2C$ showed poor material resistance to corrosion. When the carbide concentrations in the aluminium composites were increased from 2% to 4%, the following corrosion behavior is observed. Al4$Mo_2C$ and Al4TiC showed lower $R_p$ values compared to other composites (Fig. 7 (b)). The $C_{dl}$ values seen in Figure 7(d) are inversely proportional to the $R_p$ values seen in Figure 7(b). This indicates that the corrosion is higher in Al4$Mo_2C$ composite and lowest in Al4$Fe_3C$ composite. Same can be seen and verified in the optical micrographs given in Figures 3 and 4. The $R_p$ and $C_{dl}$ values are in good agreement with the micrographs obtained and hence, can be concretely stated that this corrosion analysis technique can be effectively used for powder metallurgy parts. Further, corrosion in metals usually starts at the grain boundaries and corrosion activity is promoted for powder metallurgy material due to the presence of pores. The pores present allow high pitting corrosion or localized corrosion. A decrease corrosion resistance in the composites is believed to be due to the possible microgalvanic coupling between the reinforced particles or pores and Al particles.

Further, from Figure 7 (a), it is noted that the $R_p$ values remain almost constant even though the content of TiC in aluminium matrix is increased from 1% to 4% except for few cases where $R_p$ values are higher indicating low corrosion in these specimens. Al3TiC specimens showed lower $C_{dl}$ (Figure 7 (f)) and slightly better $R_p$ when compared to Al1TiC, Al2TiC and Al4TiC. The micrographs also indicate the same that Al3TiC showed better resistance to corrosion when compared to Al1TiC, Al2TiC and Al4TiC.

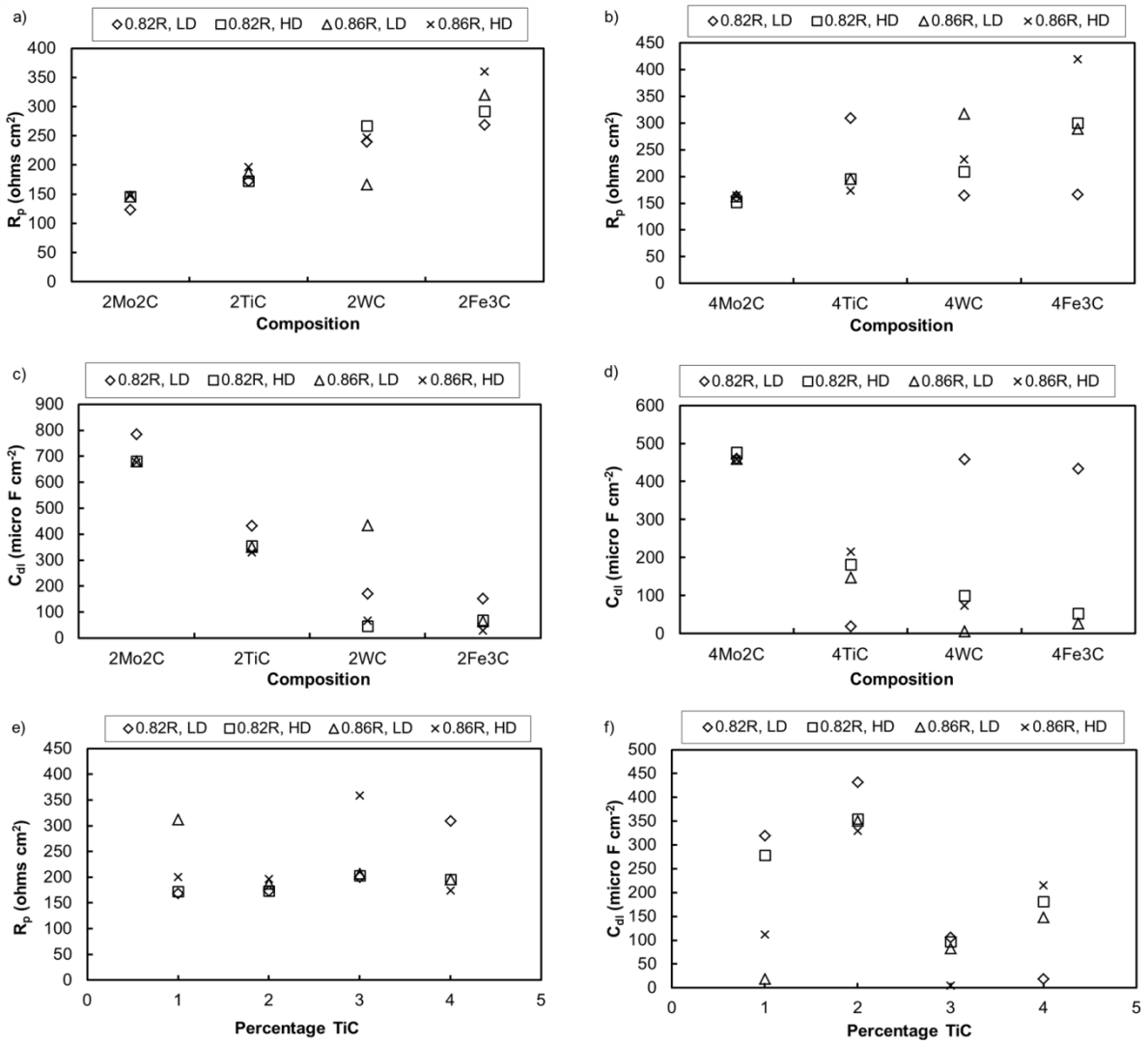


Figure 7: Variation of polarization resistance and double layer capacitance with respective carbide concentration in aluminum composites, (a and c) 2% carbide concentration, (b and d) 4% carbide concentration and (e and f) 1-4% TiC concentrations. All measurements are taken after 2 hours of immersion.

Further, the effect of initial relative density and percentage deformation is discussed here. Two preforms of 0.82 relative density and 0.86 relative density of each composite is taken and deformed to different height strain, low deformed and high deformed. It can be seen from Figure 7 that the higher initial relative density preform and highly deformed specimen showed greater material resistance to corrosion. This is clearly evident in Figure 7 (a-d) for Al2$Fe_3C$, Al2TiC, Al4WC and Al4$Fe_3C$. The effect of initial relative density and final height strain is almost negligible in $Mo_2C$ reinforced aluminium composites, however, their effect is prominent in WC

and $Fe_3C$ reinforced aluminum composites. This also ties clearly with the micrographs present in Figures 3 and 4. Similar behavior is found when the TiC content is increased from 1 to 3%, however, the same is not true for 4% TiC content.

The presence of reinforcement in the matrix increases cathode to anode ratio in the composite, resulting in the formation of pits during localized corrosion. The β-parameter can be used to study the pitting corrosion. A higher β values indicates low corrosion and a low β values indicates higher corrosion. Figure 8 gives the variation of β for different composites tested in this research work with initial relative density and different levels of height strain. It is seen that β values are lower for Al4$Mo_2C$ and Al2$Mo_2C$ composite compared to other composites. It can be noted that the pitting corrosion resistance offered by the specimen is higher in Al4$Fe_3C$ and Al2$Fe_3C$. Further, Al3TiC showed lower β values when compared to other TiC reinforced aluminium composites. It can be noted that apart from $Mo_2C$ reinforced aluminium composite, the initial relative density and low deformed Al4WC and Al4$Fe_3C$ showed very high pitting corrosion.

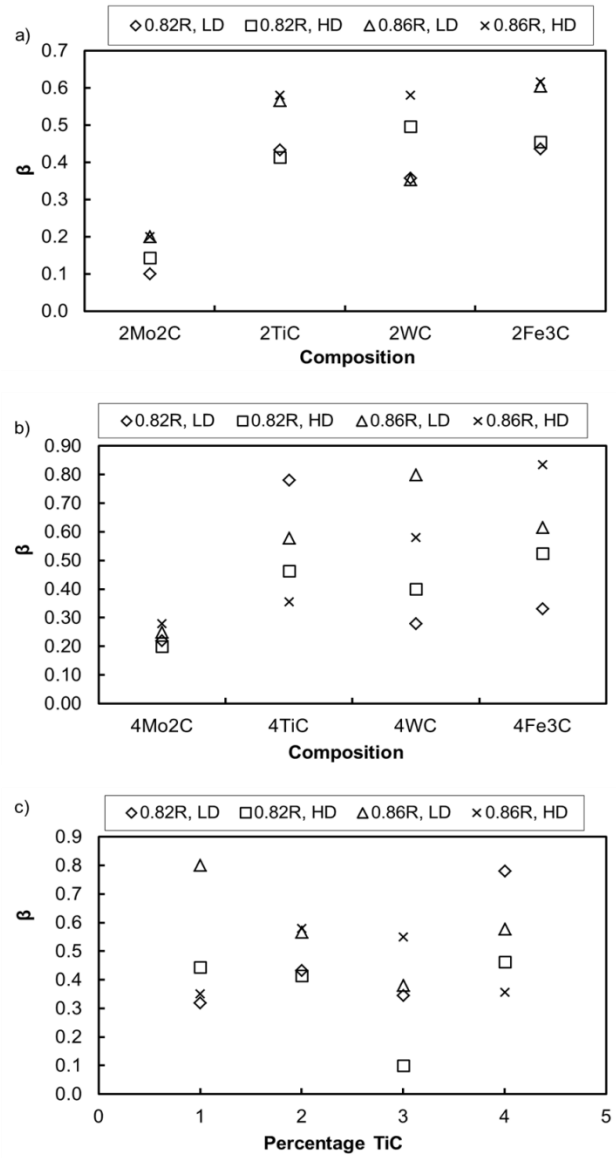


Figure 8: Variation of β-parameter with respective carbide concentration in aluminum composites, (a) 2% carbide concentration, (b) 4% carbide concentration and (c) 1-4% TiC concentrations. All measurements are taken after 2 hours of immersion.

From Figure 8 it can be noted that the β parameter is higher for higher initial relative density preforms and higher height strained preforms, except for Al4TiC composites. Higher initial relative density preforms usually archives higher final density after even secondary deformation and many researchers have presented the same [1-4]. This means that the number of pores present is less when final density attainment is high. Further, highly deformed specimen has lower number of pores in comparison to lower height strain specimens. Since the corrosion

specimens are taken from the center of the specimen, the pores present are usually round and spherical. These pores act as second phase particles and promote pitting corrosion. Hence, less number of pores are present in higher initial relative density and higher height strained specimens is the reason for high β values of these specimens suggesting lower pitting corrosion. Same can be seen in Figures 3 and 4.

## 4. Conclusion

The corrosion behaviors of Al1TiC, Al2TiC, Al3TiC, Al4TiC, Al2WC, Al4WC, Al2$Fe_3C$, Al4$Fe_3C$, Al2$Mo_2C$ and Al4$Mo_2C$ were studied in this research work. The following conclusions are drawn;

- The micrographs and electrochemical measurement strongly show that the $Mo_2C$ reinforced aluminium composites has very poor material resistance to corrosion. $Mo_2C$ reinforced aluminium composites further showed strong pitting corrosion irrespective of initial relative density and final height strain. It is noted that 2$Fe_3C$ and 4$Fe_3C$ reinforced aluminium metal matrix composite showed better corrosion resistance.
- The corrosion behavior is strongly dependent on the surface porosity. As expected, it was seen that higher porosity specimen produced lower corrosion resistance.
- The galvanostatic pulse technique using a typical three cell electrode configuration is utilized in this study to study the corrosion behavior of powder metallurgy materials. It is strongly noted that this technique can be successfully used for such studies.

## Reference


[1] Sahin Y. Preparation and some properties of SiC particle reinforced aluminium alloy composites. Mater Des 2003;24:671-9.

[2] Eslamian M, Rak J, Ashgriz N. Preparation of aluminium/silicon carbide metal matrix composites using centrifugal atomization. Powder Technology 2008;184:11-20.

[3] Narayanasamy R, Senthilkumar V, Pandey KS. Effect of titanium carbide particle addition on the densification behaviour of sintered P/M high strength steel preforms during cold upset forming. Mater Sci Eng A 2007;456:180-8.

[4] Zhang XQ, Peng YH, Li MQ, Wu SC, Ruan XY. Study of workability limits of porous materials under different upsetting conditions by compressible rigid plastic finite element method. Journal of Materials Engineering and Performance 2009;9:164-169.

[5] Gabe DR. Corrosion protection of sintered metal parts. Powder metallurgy 1977:20;227-231.

[6] Nash MS. Surface treatment for corrosion protection of sintered iron parts. Powder metallurgy 1990:33(4);22-23.

[7] Jinsun L, Hotta M, Mori Y. Improved corrosion resistance of a high-strength Mg-Al-Mn-Ca magnesium alloy made by rapid solidification powder metallurgy. Materials Science and Engineering A 2012:544;10-20.

[8] Dobrzanski LA, Wlodarczyk A, Adamiak M. Structure, properties and corrosion resistance of PM composite materials based on EN AW-2124 aluminium alloy reinforced with the $Al_2O_3$ ceramic particles. Journal of Materials Processing Technology 2005:162-163;27-32.

[9] Marchiori R, Maliska AM, Borges PC, Klein AN, Muzart. Corrosion study of plasma sintered unalloyed iron: The influence of porosity sealing and Ni surface enrichment. Materials Science and Engineering A 2007:467;159-164.

[10] Neubert V, Smola B, Stulikova I, Bakkar A, Reuter J. Microstructure, mechanical properties and corrosion behavior of dilute Al-Sc-Zr alloy prepared by powder metallurgy. Materials Science and Engineering A 2007:464;358-364.

[11] Mamatha GP, Pruthviraj RD, Ashok SD. Weight loss corrosion studies of aluminium-7075 metal matrix composites reinforced with SiC particulates in HCl solution. International Journal of Research in Chemistry and Environment 2011:1;85-88.

[12] Etaat M, Emamy M, Ghambari M, Fadaei E. Surface treatment and nickel plating of iron powder metallurgy parts for corrosion protection. Materials and Design 2009:30;3560-3565.

[13] Leisner P, Leu RC, Moller P. Electroplating of porous PM compacts. Powder metallurgy 1997:40;207-210.

[14] Wick C, Veilleux RF. Materials finishing and coating tool and manufacturing engineers hand book. Society of Manufacturing Engineers 1985.

[15] Beiss P. Steam treatment of sintered parts. Powder metallurgy 1991:34;173-177.

[16] Chenghong Y, Hongyuan F, Ji X, Guo Z, Dong G, Wan W, Chen H. Effect of WC content on the microstructures and corrosion behavior of Ti(C, N) based cermets. Ceramics International 2013;39:503-509.

[17] Chandramouli R, Kandavel TK, Shanmugasundaram D, Kumar TA. Deformation, densification and corrosion studies of sintered powder metallurgy plain carbon steel preforms. Materials and Design 2007: 28;2260-2264.

[18] Lei Z, Maicang Z, Jianxin D. Hot corrosion behavior of powder metallurgy Rene95 nickel-based superalloy in molten NaCl-$Na_2SO_4$ salts. Materials and Design 2011:32;1981-1989.

[19] Kumar SMS, Rao KP, Girish DP. Corrosion rate and tensile strength of aluminium/SiC metal matrix composites in seawater. International Journal of Advanced Engineering Research and Studies 2012:1;313-315.

[20] Alaneme KK, Bodunrin MO. Corrosion behavior of Alumina reinforced aluminium (6063) metal matrix composites. Journal of Minerals and Materials Characterization and Engineering 2011:10;1153-1165.

[21] Bobic B, Mitrivic S, Babic M, Bobic I. Corrosion of aluminium and zinc-aluminium alloys based metal matric composites. Tribology in Industry 2009:31;44-52.

[22] Sharma SC. A study on stress corrosion behavior of Al6061/albite composite in higher temperature acidic medium using autoclave. Corrosion Science 2001:43;1877-1889.

[23] Scully JR, Corrosion 2000:56;199-218.

[24] Deo RN, Birbilis N, Cull JP. Measurement of corrosion in soil using galvanostatic pulse technique. Corrosion Science 2014:80;339-349.

[25] Sherif ME, Almajid AA, Latif FH, Junaedi H. Effects of graphite on the corrosion behavior of aluminium graphite composite in sodium chloride solutions. International Journal of Electrochemical Science 2011:6;1085-1099.

[26] Birbilis N, Nairn KM, Forsyth M. Corrosion Science 2003:43;1895-1902.

[27] Lu C, Peiyu Y. Corrosion Science 2000:42;675-686.

[28] M.G. Zuhair, M.A.Q. Amro, Corrosion behavior of powder metallurgy aluminium alloy 6061/$Al_2O_3$ metal matrix composites, The 6$^{th}$ Saudi Engineering Conference, Dhahram, 2002;5:271-280.

[29] R.N. Deo, Geophysical methods for assessment of soil corrosivity, PhD thesis, School of Geosciences, Monash University, Melbourne, Australia, 2013.

[30] N. Birbilis, B.W. Cherry, Monitoring the corrosion and remediation of reinforced concrete on-site: An alternative approach, Materials and Corrosion, 2005;56(4):237-243.